Lattice Mesoscopic Model of Dynamically Heterogeneous Fluids

A. Lamura
Istituto Applicazioni Calcolo, CNR, Sezione di Bari, Via Amendola 122/D, 70126 Bari, Italy

S. Succi
Istituto Applicazioni Calcolo, CNR, Viale del Policlinico 137, 00161 Roma, Italy

(Received 7 February 2005; revised manuscript received 18 July 2005; published 21 November 2005)

We introduce a mesoscopic three-dimensional lattice Boltzmann model which attempts to mimic the physical features associated with cage effects in dynamically heterogeneous fluids. To this purpose, we extend the standard lattice Boltzmann dynamics with self-consistent constraints based on the nonlocal density of the surrounding fluid. The resulting dynamics exhibits typical features of dynamic heterogeneous fluids, such as non-Gaussian density distributions and long-time relaxation. Because of its intrinsically parallel dynamics, and absence of statistical noise, the method is expected to compute significantly faster than molecular dynamics, Monte Carlo, and lattice glass models.

DOI: 10.1103/PhysRevLett.95.224502 PACS numbers: 47.11.+j, 05.70.Ln, 61.43.−j

Very slow relaxation and long equilibration times are a typical feature of complex fluids, such as supercooled liquids, polymers and others [1,2]. The numerical study of these complex systems is usually undertaken by many-body simulation methods, such as molecular dynamics [3], Monte Carlo simulations [4], and various types of lattice "glasses" [5–10]. Since many-body simulations are computationally demanding, it is worth exploring whether the salient features of dynamic heterogeneities can be reasonably described by effective one-body techniques in the spirit of density functional theory [11]. A powerful one-body technique is the lattice Boltzmann (LB) method. The LB dynamics consists of three basic steps: Free-streaming, collisional relaxation [12], and (effective) intermolecular interactions [13]. A judicious choice of these intermolecular interactions permits us to describe the dynamics of a variety of complex flows [14]. However, applicability of LB to glassylike fluids remains an open problem [15]. A crucial aspect of the physics of complex fluids are dynamic heterogeneities and geometrical frustration, i.e., the presence of sterical constraints which reduce the phase space available to the fluid system. Real systems like colloids, or granular materials, exhibit glassy dynamics associated to jamming: Density, rather than temperature, is the dominant effect in slowing down strongly the dynamics [16]. In an attempt to model these effects, we develop a lattice Boltzmann equation (LBE) in which free-particle motion is confined to a subset of links which fulfill self-consistent dynamic constraints on the surrounding fluid density. The presence of these kinetic constraints on free-particle motion leads to drastic departures from simple fluid behavior, such as long-time relaxation and non-Gaussian density fluctuations. We begin by considering a standard LBE with a single relaxation time [17,18]:

$$f_i(\mathbf{r}, t) - f_i(\mathbf{r}_i, t - \Delta t) = -\omega \Delta t [f_i - f_i^e](\mathbf{r}_i, t - \Delta t), \tag{1}$$

where Δx and Δt are space and time steps, respectively, $f_i(\mathbf{r}, t) \equiv f(\mathbf{r}, \mathbf{v} = \mathbf{c}_i, t)$ is a discrete distribution function of particles at site $\mathbf{r}$ and at time t moving along the direction i of a lattice, with discrete speed $\mathbf{c}_i$, and $\mathbf{r}_i \equiv \mathbf{r} - \mathbf{c}_i \Delta t$. The previous equation can be seen as the combination of collision and streaming steps. In the collision, the distribution functions f_i relax to a local equilibrium f_i^e in a time lapse of the order of ω^{-1}, such that the distribution function after a collision f_i^c is:

$$f_i^c(\mathbf{r}_i, t - \Delta t) = f_i(\mathbf{r}_i, t - \Delta t) - \omega \Delta t [f_i - f_i^e](\mathbf{r}_i, t - \Delta t). \tag{2}$$

The distribution function f_i^c then streams freely to neighbor sites, so that the updated values are just the shifted postcollisional distributions:

$$f_i(\mathbf{r}, t) = f_i^c(\mathbf{r}_i, t - \Delta t). \tag{3}$$

The large-scale behavior of system depends crucially on the form of the local equilibria. In the present Letter, the equilibrium distribution functions f_i^e are expressed as

$$f_i^e(\mathbf{r}, t) = w_i \rho(\mathbf{r}, t), \tag{4}$$

where w_i is a set of lattice-dependent weights normalized to unity. The local density $\rho(\mathbf{r}, t)$ in Eq. (4) is obtained by a direct summation upon all discrete distributions:

$$\rho(\mathbf{r}, t) = \sum_i f_i(\mathbf{r}, t). \tag{5}$$

Since the local equilibria do not depend on the local fluid speed, the only conserved quantity is the fluid density, which means that in the continuum limit, the system obeys a simple diffusion equation: $\partial_t \rho(\mathbf{r}, t) = D \nabla^2 \rho(\mathbf{r}, t)$ with diffusion constant $D = (\Delta x)^2 / 3 \Delta t (\frac{1}{\omega \Delta t} - \frac{1}{2})$. Should flow phenomena be of interest as well, we should just add a quadratic term in the flow speed to the local equilibrium distribution functions (4). In the following, we shall refer to

a three-dimensional cubic lattice of size $L \times L \times L$ with $\mathbf{c}_0 = (0, 0, 0)$ and $\mathbf{c}_i = (\pm\Delta x/\Delta t, 0, 0)$, $(0, \pm\Delta x/\Delta t, 0)$, $(0, 0, \pm\Delta x/\Delta t)$, $i = 1, 2, \ldots, 6$. In this case $w_0 = 1/3$ and $w_i = 1/9$ for $c_i = \Delta x/\Delta t$, $i = 1, 2, \ldots, 6$. We enforce sterical constraints which have proven to be effective to capture the physics of glassy systems where density is the dominant observable [2,8]. Kinetic constraints on the evolution of the system are enforced by the following functional rule: Propagation from a site $\mathbf{r}$ to one of its 6 neighbors $\mathbf{r}'$ is permitted only if the *nonlocal* densities $\rho_{\mathrm{nl}}(\mathbf{r}) = \sum_{i=1}^{6} \rho(\mathbf{r} + \mathbf{c}_i\Delta t)$ and $\rho_{\mathrm{nl}}(\mathbf{r}') = \sum_{i=1}^{6} \rho(\mathbf{r}' + \mathbf{c}_i\Delta t)$, prior and after streaming, respectively, both lie below a given density threshold, S. In the limit $S \to \infty$, the effective propagator taking the system from site $\mathbf{r}$ at time t to site $\mathbf{r}'$ at time $t + \Delta t$, reduces to the standard free-particle form, $G_i(\mathbf{r}, \mathbf{r}'; \Delta t) = \delta(\mathbf{r}' - \mathbf{r} - \mathbf{c}_i\Delta t)$. In the opposite limit, $S \to 0$, no motion is allowed and $G_i \to \delta(\mathbf{r}' - \mathbf{r})$ at all sites, corresponding to structural arrest. It is therefore clear that the ratio $\langle\rho\rangle/S$ ($\langle\ldots\rangle$ stands for a spatial average), serves as a control parameter driving the system from the purely diffusive to the structural arrest regime. The above rule is implemented as follows: (1) Initialize the system by randomly choosing N lattice sites and set them at a local density ρ_0. The remaining L^3-N sites are set at density 0. The average density in the system is then $\langle\rho\rangle = \chi\rho_0 \leq \rho_M$, where $\rho_M = \rho_0$ is the maximum possible average density in the system, and $\chi = N/L^3$ is the concentration of "loaded" sites; (2) Compute local densities $\rho(\mathbf{r})$ via Eq. (5); (3) Compute the equilibrium distribution functions f_i^e via Eq. (4); (4) Perform the collision (2) on all the lattice sites to compute f_i^c; (5) Look for *all* the lattice sites $\mathbf{r}^*$ such that $\sum_{i=1}^{6} \rho(\mathbf{r}^* + \mathbf{c}_i) < S$ where S is a fixed threshold; (6) Perform a prestreaming, according to Eq. (3), of the f_i^c computed at step 4 *only* along links emanating from the lattice sites $\mathbf{r}^*$ and pointing towards neighbor sites $\mathbf{r}^*$; (7) Compute again local densities $\rho^*(\mathbf{r})$ on *all* the lattices sites; (8) Look for *all* the lattice sites $\mathbf{r}^{**}$ such that $\sum_{i=1}^{6} \rho^*(\mathbf{r}^{**} + \mathbf{c}_i) < S$; (9) Perform the effective streaming step of the f_i^c computed at step 4 only along links from $\mathbf{r}^*$ to $\mathbf{r}^{**}$ sites (these links will be denoted as *active* ones), otherwise the f_i^c are not moved; (10) Go to (2). The LB scheme described above is intrinsically distinct from those used for nonideal fluids. Indeed, while the latter include potential energy via effective interactions which leave the free-propagator (kinetic energy) unaffected, in our case the interactions alter the structure of the kinetic energy operator.

We have simulated two lattice sizes, $L = 16$ and 32, with $\Delta x = \Delta t = 1$. We changed ω in the range $[0.1:1]$ and did not find any dependence of results on its specific value. Thus, we set $\omega = 0.1$. We used $\rho_0 = 0.5$ and $S = 1.5$, corresponding to single site density threshold $\rho_S = S/6 = 0.25$. Keeping ρ_0 fixed, we chose the smallest value of S such as to ensure sluggish dynamics at high densities, while still allowing the system to be uniform at low densities. By running several simulations with $\rho_0 = 0.5$, we have found that for $S \gtrsim 1$ the system evolves by diffusive smoothing of the density gradients towards a long-time state characterized by a uniform density pattern when $\langle\rho\rangle \lesssim 0.03$. Moreover, when $S \gtrsim 2.3$, the system does not show any singular behavior for densities smaller than the maximum possible one, ρ_M (see below). This latter feature is also observed by increasing ρ_0 while keeping $S = 1.5$. This is because, by increasing ρ_0 at a fixed average density $\langle\rho\rangle$, the number N of lattice sites to be initialized with density ρ_0 decreases, and consequently it becomes more difficult for the kinetic constraints to be effective. In conclusion, the system seems to exhibit a nonsmooth transition from diffusive to sluggish behavior as the reduced density $\lambda = \langle\rho\rangle/\rho_S$ is increased.

This is shown in Fig. 1, where we plot the order parameter $m = (\rho_{\max}\text{-}\rho_{\min})/\rho_0$ as a function of λ by keeping $\langle\rho\rangle = 0.12$ and $\rho_0 = 0.5$ fixed and varying S. Here, $\rho_{\max}$ and $\rho_{\min}$ are the maximum and minimum values of ρ, respectively, at steady state. The values of m were averaged over 50 independent runs on systems of size $L = 32$. The simulations yield $m \simeq 0$ for $\lambda \lesssim 0.36$, indicating a purely diffusive behavior, then m undergoes a sharp rise and the system enters the sluggish regime. At values of $\lambda \gtrsim 1.44$, the system is nearly frozen in its initial configuration and the order parameter m settles down to 1 since $\rho_{\max} = \rho_0$ and $\rho_{\min} = 0$. Figure 1 clearly indicates the existence of three distinct regimes, namely, a low-density diffusive regime at $\lambda < \lambda_D \simeq 0.36$, a high-density frozen regime at $\lambda > \lambda_F \simeq 1.44$, and a sluggish regime at intermediate densities $\lambda_D < \lambda < \lambda_F$. Since the initial density of occupied sites is ρ_0, the initial nonlocal density $\rho_{nl}(\mathbf{r}) = \sum_{i=1}^{6} \rho(\mathbf{r} + \mathbf{c}_i\Delta t)$ can be at most $6\rho_0$. Therefore, the con-

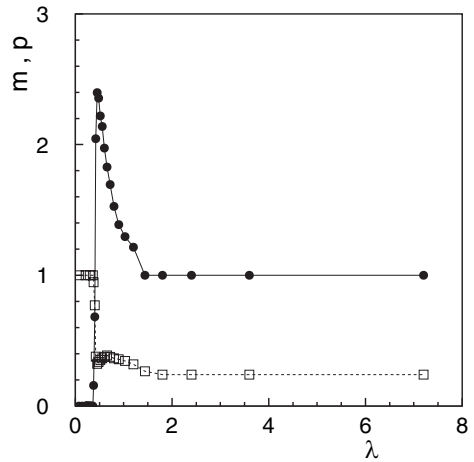

FIG. 1. The order parameter m (●) as a function of the reduced density λ with $\rho_0 = 0.5$, $\langle\rho\rangle = 0.12$, and $L = 32$. Also shown is the steady-state value of participation number p (□), defined as $p = 1/(L^3 \sum_{i=1}^{L^3} p_i^2)$, with $p_i = \rho(\mathbf{r}_i)/(\chi L^3\rho_0)$ being the occupation probability of the site i. By definition $p(t = 0) = \chi$ and $p = 1$ in the case of uniform distribution. This plot shows that $\chi < p < 1$ indicating that the system never becomes more localized than in the initial configuration.

dition for a purely diffusive behavior is $6\rho_0 \lesssim S \Rightarrow \lambda \lesssim 0.24$, which is in a reasonable agreement with the value provided by simulations. The value of λ marking the transition from the glassy to the frozen regime can be determined by considering that the average initial nonlocal density is $\rho_{\rm nl}(\mathbf{r}) = 6\chi\rho_0$. When $6\chi\rho_0 \gtrsim S \Rightarrow \lambda \gtrsim 1.0$, the system is likely to be frozen. This underestimates the value obtained from simulations, but the value of the order parameter $m(1) \simeq 1.3$, well below its maximum $m \simeq 2.4$, indicates that the system is approaching the frozen regime. We choose $\lambda = 0.48$, in order to select a regime with a clear departure from ideal fluid behavior [$m(0.48) \simeq 2.35$]. For this set of parameters the system evolves from the initial random configuration forming some clusters until, at long times, it gets arrested in one of the highly heterogeneous states. The arrest time decreases with increasing average density $\langle\rho\rangle$. To analyze the qualitative difference with respect to the simple diffusion dynamics, we also inspected the probability distribution functions of density. It is observed that the system, which starts from a two-peak distribution at $\rho = 0$ and ρ_0, rapidly fills up all available values in the range [0:1.1]. At long times there is a sharp peak at $\rho \simeq 0.05$, which corresponds to the background density and the distribution is nonuniform everywhere else, with a pronounced shoulder at $\rho \simeq 0.1$.

We computed the time autocorrelation function

$$h(t) = \frac{\langle\langle \delta\rho(t + t_0)\delta\rho(t_0)\rangle\rangle}{\langle\langle \delta\rho(t_0)\delta\rho(t_0)\rangle\rangle}, \qquad (6)$$

where $\langle\langle \ldots \rangle\rangle$ denotes an average over space and initial times t_0 and $\delta\rho(t) = \rho(t) - \langle\rho\rangle$. The plots for several values of the initial density $\langle\rho\rangle$ are shown in Fig. 2 for the case $L = 32$. Data were obtained by averaging over 50 independent runs for each value of $\langle\rho\rangle$. For very small values of $\langle\rho\rangle$, the system goes to a final state with uniform density and $h(t)$ relaxes to zero. By increasing $\langle\rho\rangle$, $h(t)$ starts forming a plateau and stays close to the unit value for a time span which increases rapidly with increasing mean density $\langle\rho\rangle$. Even at high densities, the correlator does not show the ''two-step'' relaxation behavior often found in glassy materials. We believe that this is due the absence of a rattling motion in our model [a similar behavior is found in the Kob-Andersen (KA) model [5] for lattice glasses].

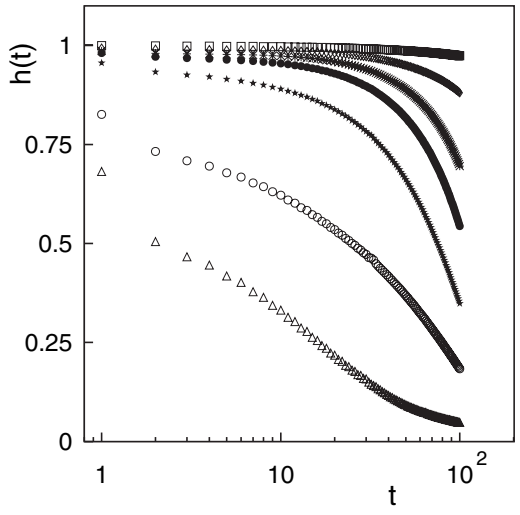

FIG. 2. Autocorrelation function $h(t)$ as a function of time t for $\langle\rho\rangle = 0.08(\triangle)$, $0.09(\bigcirc)$, $0.10(\star)$, $0.11(\bullet)$, $0.12(*)$, $0.18(\diamond)$, $0.30(\square)$ with $\rho_0 = 0.5$, $S = 1.5$, and $L = 32$.

We compared our results with the predictions of mode-coupling theory (MCT) [19]. MCT predicts a power-law time decay away from the plateau. We therefore tried to fit the short-time behavior of the function $h(t)$ with a power law of the form f-Bt^b, where f, B, and b are fitting parameters. Such a power-law decay is indeed reproduced by our simulations in the high-density regime where from all the fits we find f very close to 1 (to within 10^{-3}) as in the KA model [5]. The coefficient B decreases at increasing values of $\langle\rho\rangle$ varying in the range $[4 \times 10^{-5}{:}3 \times 10^{-4}]$. At variance with MCT predictions, the power-law exponent b is not independent of density but decreases at increasing values of $\langle\rho\rangle$ varying in the range [0.8:1.0]. This density dependence of b is found also in the KA model [5] with b decreasing at increasing values of $\langle\rho\rangle$ varying in the range [0.8:1.1], which is consistent with our results. In MCT the decay at longer times is predicted to be a stretched exponential, $h(t) \propto \exp[-(t/\tau)^\beta]$, where the exponent β is density-independent and the relaxation time τ is the relevant physical parameter. Indeed, this time scale increases strongly as density is increased (MCT predicts a singular behavior for τ at a density smaller than the maximum one ρ_M). Chemically different materials relax in a qualitatively similar manner with relaxation functions obeying the Kohlraush-William-Watts function $\exp[-(t/\tau)^\beta]$ [20]. We fitted successfully $h(t)$ at long times for $\langle\rho\rangle \geq 0.12$ by using a stretched exponential with τ and β as fitting parameters and found that the inverse relaxation time $1/\tau$ vanishes at a critical density $\rho_c = 0.412 \pm 0.010$, with power law $6(\rho_c - \langle\rho\rangle)^{\gamma_c}$, being $\gamma_c = 4.68$ (in the KA model the critical exponent γ_c is ~ 5 [5]), while the stretching exponent β is density-dependent. MCT predicts such a power law behavior for the relaxation time with a system-dependent exponent γ_c [21]. It is remarkable that, despite the density dependence, we find numerically that $\beta(\langle\rho\rangle) \simeq b(\langle\rho\rangle)$, as predicted in MCT for the time dependence of the autocorrelation function [22]. We stress that the critical value ρ_c is smaller than the maximum density ρ_M, corresponding to a fully-loaded lattice. The plot of the relevant physical quantity $1/\tau$ as a function of $\rho_c - \langle\rho\rangle$ is shown in Fig. 3, where we also report the fitting values of $1/\tau$ for the system size $L = 16$. Also in this case, we found that $1/\tau$ vanishes with a power-law behavior and the estimated critical density is 0.405 ± 0.029, which is consistent with ρ_c within the error range, with no significant lattice size effect. This suggests a singular behavior at about $\langle\rho\rangle = 0.412$. We also inspected the ratio F of active lattice links to the total number $6L^3$ of lattice links. This quantity can be viewed as a measure of the degree of glassiness, as observed in kinetically con-

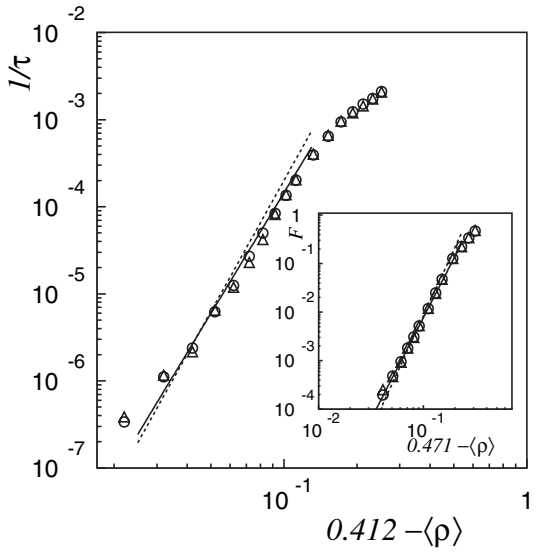

FIG. 3. Inverse relaxation time $1/\tau$ as a function of $0.412\text{-}\langle\rho\rangle$ for $\rho_0 = 0.5$, $S = 1.5$, and $L = 16(\triangle), 32(\bigcirc)$. The full line has slope 4.68. In the inset the fraction F of active links versus $0.471\text{-}\langle\rho\rangle$ is shown for the same parameters. The full line has slope 4.19. For a comparison we plotted the results of the KA model by using dashed lines.

strained lattice glass models [10], since we expect the relaxation time τ to diverge in the limit $F \to 0$. In the limit $\langle\rho\rangle \to 0$, $F \to 1$ since the kinetic constraints do not play any role. When $\langle\rho\rangle \to \rho_c$, we expect $F \to 0$ since in this limit the kinetic constraints are very effective in slowing down the dynamics [5].

In the inset of Fig. 3 we plot the steady-state values of F, averaged over 50 runs, for each value of $\langle\rho\rangle$. We found that F vanishes at a critical density $\rho_c' = 0.471 \pm 0.005$, with power law $120(\rho_c' - \langle\rho\rangle)^{\gamma_c'} \doteq$, being $\gamma_c' = 4.19$. In the case of the KA model, a similar power law is found with critical exponent $\gamma_c' \sim 4.7$ [5]. In the same inset we also report the values of F for the system size $L = 16$. Also in this case we found that F vanishes with a power-law behavior and the estimated critical density is 0.482 ± 0.016, which is consistent with ρ_c' within the error range, and no significant lattice size effect. It is interesting to note that $\rho_c' \simeq \rho_c$, supporting the conclusion that our model shows singular behavior at a density smaller than the maximum possible one, ρ_M.

Summarizing, we have introduced a mesoscopic LB model which appears to reproduce *some* physical features of dynamically heterogeneous fluids, such as sluggish relaxation and continuum density distributions. To this purpose, the standard LB dynamics has been augmented with self-consistent constraints based on the nonlocal density of the surrounding fluid. A typical run on a 32^3 lattice (4 times larger than typical lattice glass simulations [5,7]) takes just a few minutes on a 2.4 GHz Intel Xeon processor.

Illuminating discussions with K. Binder, W. Kob, E. Marinari, and G. Parisi are kindly acknowledged.

[1] For reviews, see, e.g., C. A. Angell, Science **267**, 1924 (1995); H. Sillescu, J. Non-Cryst. Solids **243**, 81 (1999); S. C. Glotzer, J. Non-Cryst. Solids **274**, 342 (2000); P. G. Debenedetti and F. H. Stillinger, Nature (London) **410**, 259 (2001).
[2] J. P. Garrahan and D. Chandler, Phys. Rev. Lett. **89**, 035704 (2002).
[3] W. Kob and H. C. Andersen, Phys. Rev. Lett. **73**, 1376 (1994).
[4] K. Binder, J. Baschnagel, and W. Paul, Prog. Polym. Sci. **28**, 115 (2003).
[5] W. Kob and H. C. Andersen, Phys. Rev. E **48**, 4364 (1993).
[6] G. Biroli and M. Mezard, Phys. Rev. Lett. **88**, 025501 (2002).
[7] M. Pica Ciamarra, M. Tarzia, A. de Candia, and A. Coniglio, Phys. Rev. E **67**, 057105 (2003); **68**, 066111 (2003).
[8] F. Ritort and P. Sollich, Adv. Phys. **52**, 219 (2003).
[9] C. Toninelli, G. Biroli, and D. S. Fisher, Phys. Rev. Lett. **92**, 185504 (2004).
[10] E. Bertin, J.-P. Bouchaud, and F. Lequeux, Phys. Rev. Lett. **95**, 015702 (2005).
[11] J. K. Percus, Mol. Phys. **100**, 2417 (2002).
[12] F. J. Higuera, S. Succi, and R. Benzi, Europhys. Lett. **9**, 345 (1989).
[13] R. Benzi, S. Succi, and M. Vergassola, Phys. Rep. **222**, 145 (1992); D. A. Wolf-Gladrow, *Lattice Gas Cellular Automata and Lattice Boltzmann Models* (Springer-Verlag, New York, 2000).
[14] X. Shan and H. Chen, Phys. Rev. E **47**, 1815 (1993); **49**, 2941 (1994); M. R. Swift, W. R. Osborn, and J. M. Yeomans, Phys. Rev. Lett. **75**, 830 (1995); A. Lamura, G. Gonnella, and J. M. Yeomans, Europhys. Lett. **45**, 314 (1999); A. C. J. Ladd, J. Fluid Mech. **271**, 285 (1994).
[15] A. Lamura and S. Succi, Eur. Phys. J. B **39**, 241 (2004); Physica A (Amsterdam) **325**, 477 (2003); Int. J. Mod. Phys. B **17**, 145 (2003).
[16] M. D. Ediger, Annu. Rev. Phys. Chem. **51**, 99 (2000).
[17] P. Bhatnagar, E. P. Gross, and M. K. Krook, Phys. Rev. **94**, 511 (1954).
[18] Y. H. Qian, D. d'Humieres, and P. Lallemand, Europhys. Lett. **17**, 479 (1992).
[19] U. Bengtzelius, W. Götze, and A. Sjölander, J. Phys. C **17**, 5915 (1984); E. Leutheusser, Phys. Rev. A **29**, 2765 (1984).
[20] J. Jäckle, Rep. Prog. Phys. **49**, 171 (1986).
[21] W. Kob (private communication); For a comparison between MCT and real systems see, e.g., W. Götze and J. Sjögren, Rep. Prog. Phys. **55**, 241 (1992).
[22] M. Fuchs, J. Non-Cryst. Solids **172**, 241 (1994).